

## Cloaking mechanism with antiphase plasmonic satellites

Mário G. Silveirinha,<sup>1,2</sup> Andrea Alù,<sup>1,3</sup> and Nader Engheta<sup>1,\*</sup>

<sup>1</sup>*Department of Electrical and Systems Engineering, University of Pennsylvania, Philadelphia, Pennsylvania 19104, USA*

<sup>2</sup>*Department of Electrical Engineering–Instituto de Telecomunicações, Universidade de Coimbra, 3030 Coimbra, Portugal*

<sup>3</sup>*Department of Electrical and Computer Engineering, University of Texas at Austin, Austin, Texas 78712-0240, USA*

(Received 20 May 2008; revised manuscript received 14 October 2008; published 12 November 2008)

In this work we theoretically demonstrate the possibility of cloaking a given object by surrounding it with a finite collection of suitably dimensioned, discrete “antiphase” plasmonic scatterers. It is shown that the total scattering from the object may approximately be canceled by the currents induced on a finite number of the plasmonic “satellite” scatterers, effectively making the whole system invisible to an external observer. Unlike other approaches, the proposed solution allows one to cloak a given object in a noninvasive manner since the antiphase satellites, being finite in number, do not need to fully cover and be in direct contact with the cloaked object.

DOI: [10.1103/PhysRevB.78.205109](https://doi.org/10.1103/PhysRevB.78.205109)

PACS number(s): 78.66.Sq, 41.20.Jb, 42.79.-e

### I. INTRODUCTION

When an electromagnetic wave illuminates an object, part of the energy of the incoming beam is scattered in the whole space, making its presence detectable to neighboring observers. In many applications, such as remote sensing, radars, radomes, and medical or biological measurements, it may be desirable to drastically reduce this scattering, ideally independent of the direction of the impinging wave and the observer’s position. This general problem of “cloaking” an object or a region of space with a suitable cover that induces “invisibility” has received significant attention recently. In particular, our group has demonstrated, analytically and numerically, that when a given object is covered with a properly designed plasmonic shell then, despite the fact that its physical size increases, its total scattering cross section may drastically drop.<sup>1</sup>

Other cloaking techniques based on coordinate transformations,<sup>2–5</sup> optical conformal mapping,<sup>6</sup> and anomalous localized resonances<sup>7</sup> have also been recently suggested. These techniques are based on quite different principles from the one discussed in this work, and in general require the availability or construction of complex, highly anisotropic resonant and nonuniform materials with electrical and/or magnetic responses. On the contrary, in the “scattering-cancellation” technique<sup>1</sup> the cloak may be homogeneous and isotropic, in general independent of the wave polarization and its direction of incidence. A review and comparison of different cloaking techniques employing metamaterials and plasmonics was recently reported in Ref. 8.

The phenomenon described in Ref. 1 is a consequence of the out-of-phase polarizability of plasmonic materials, which, under suitable conditions, may compensate for and annihilate the scattering from the cloaked object. This effect enables the “tunneling” of the electromagnetic wave through (and/or around) the cloaking system and the possibility for an observer to “see through and beyond” the cloaked object at the design frequency. A related tunneling effect may also be observed in other more complex scenarios involving closed geometries.<sup>9</sup> In Refs. 10 and 11 we also demonstrated how this transparency technique may be applied at frequen-

cies for which plasmonic materials are not directly available in nature, by designing the cover as a parallel-plate metamaterial with metallic implants. In Ref. 12, moreover, we proved that the proposed transparency technique is robust against variations in the design parameters, such as variations in frequency around the design frequency or modification of size and shape of the cloaked object. In Ref. 13 we extended these concepts to collections of particles and larger objects. In Ref. 14, finally, we showed that multilayered cloaks may ensure multifrequency operation and further improved performance.

Here, following a similar principle, we discuss and analyze the idea of using “antiphase” scatterers placed near an object to achieve similar effects without the need for totally covering the object to be cloaked. Indeed, under some circumstances it may not be ideal or practically possible to fully cover the desired object with a uniform cover, and thus the technique proposed here may provide more flexibility and degrees of freedom in these situations. Moreover, it may often be difficult to realize the required plasmonic cover when the object of interest has a complex shape. Since the transparency technique proposed in Ref. 1 is shown to be based on an integral effect rather than on a resonance phenomenon,<sup>12</sup> it is expected that scattering cancellation may still be achieved using a limited number of “concentrated,” properly designed satellites provided that we can induce an analogous “negative” scattering in them. Analogous to Ref. 1, this negative scattering may be provided by materials with real part of the permittivity less than that of free space (or that of the background medium). As discussed in Refs. 1 and 12, such materials exhibit a negative polarizability; i.e., the local induced dipole moment is 180° out of phase with the impinging electric field. This provides the possibility of canceling part, if not most, of the scattered power.

The aim of this paper is to demonstrate, analytically and with full-wave simulations, that surrounding an object with a suitable agglomerate of antiphase scatterers yields an alternative, viable, and arguably simple, noninvasive cloaking mechanism. The antiphase “satellites” are designed in such a way that the collective superimposition of the scattered waves interferes destructively, making the total system “invisible” to radiation.

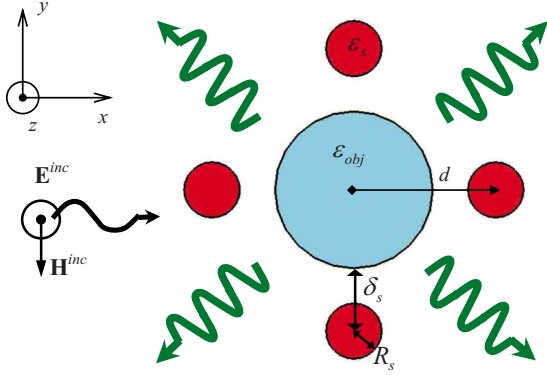


FIG. 1. (Color online) Geometry of the problem: a system formed by a dielectric cylindrical object and antiphase plasmonic scatterers (so-called satellites) illuminated by an incoming plane wave. The position and the material parameters of the satellites are optimized [using, for example, the genetic algorithm (GA)] to reduce the total scattering cross section from the whole system, inducing an effective cloaking mechanism.

## II. THEORETICAL ANALYSIS

To begin with, we will develop a theoretical model that describes approximately the scattering properties of a system formed by a given object and an agglomerate of satellites (see Fig. 1 for a representative geometry). As explained in Sec. I, the object is surrounded by a set of antiphase scatterers, which should be designed in such a way that the total scattering from the overall system is made very small due to destructive interference at all visible angles. For simplicity, it is assumed that the geometry is invariant to translations along the  $z$  direction, and that the incoming wave propagates on the  $x$ - $y$  plane, so that the problem is effectively two dimensional (2D). The electric field is assumed to be polarized along the  $z$  direction.

In order to obtain an analytical solution that may enable a qualitative description of the main features of the system, we will consider the case in which both the object and the satellites are electrically small so that their interaction may be treated as an electric dipole-type interaction. In Sec. III, we will present a general design procedure based on a full-wave electromagnetic analysis that takes into account all the interactions between the particles and the effect of higher dipole moments, and does not require that the particles be treated as electric dipoles.

Let  $\alpha_e^{(i)}$  be the electric polarizability [per unit of length (pul)] along the direction of the symmetry axis of a given particle (the  $i$ th particle). The electric dipole moment (pul) induced on the particle along the  $z$  direction is

$$p_e^{(i)} = \varepsilon_0 \alpha_e^{(i)} E_{\text{loc}}^{(i)}, \quad (1)$$

where  $E_{\text{loc}}^{(i)}$  is the local field at the particle's site  $\mathbf{r}_i$ , and is given by the superposition of the incident wave and the field scattered by the remaining particles in the system. Within the dipole approximation, the field scattered by the  $i$ th particle is

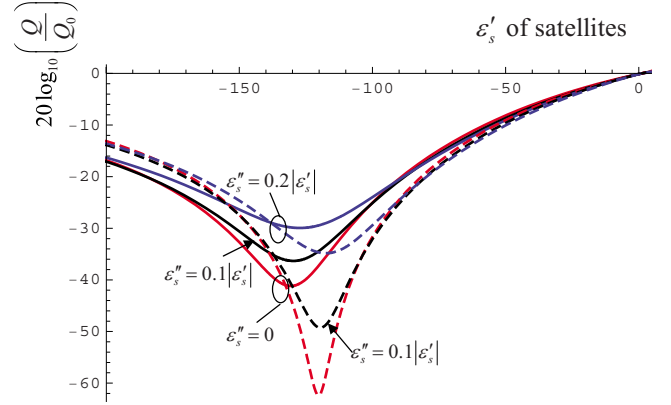


FIG. 2. (Color online) Total scattering linewidth  $Q$  for a 2D system formed by a circular object and four antiphase satellites (see Fig. 1), as a function of the real part of the complex permittivity of the satellites,  $\varepsilon_s = \varepsilon'_s + i\varepsilon''_s$ , and different values of the loss tangent. Solid lines: full-wave results; dashed lines: analytical model.  $Q$  is normalized to the scattering linewidth of the object standing alone in free space,  $Q_0$ . The object has permittivity  $\varepsilon_{\text{obj}} = 4.0$  and diameter  $D = \lambda_0/6$ . The radius of the satellites is  $R_s = 0.05D$  and the distance between the center of the object and the center of the satellites is  $d = 0.6D$ .

$$E_s^{(i)}(\mathbf{r}) \approx k_0^2 \Phi_0(\mathbf{r} - \mathbf{r}_i) \frac{p_e^{(i)}}{\varepsilon_0}, \quad (2)$$

where  $\mathbf{r} = (x, y)$  represents a generic point of space,  $k_0 = \omega \sqrt{\varepsilon_0 \mu_0}$  is the free-space wave number, and  $\Phi_0(\mathbf{r} - \mathbf{r}_i) = (i/4) H_0^{(1)}(k_0 |\mathbf{r} - \mathbf{r}_i|)$  is the fundamental solution of Helmholtz's equation, with  $H_n^{(1)}$  as the Hankel function of first kind and order  $n$ . Suppose that the considered system of particles is illuminated by an incoming wave with electric field  $E_{\text{inc}}(\mathbf{r})$ . In these conditions, it is clear that the local field at the  $i$ th particle's site is

$$E_{\text{loc}}^{(i)} = E_{\text{inc}}(\mathbf{r}_i) + \sum_{j \neq i} C_{i,j} \frac{p_e^{(j)}}{\varepsilon_0}, \quad C_{i,j} = k_0^2 \Phi_0(\mathbf{r}_i - \mathbf{r}_j), \quad (3)$$

i.e., the local field depends on the incident field as well as on the electric dipole moments induced in all the other particles of the system. Substituting the above expression into Eq. (1), it is found that the induced dipole moments  $p_e^{(i)}$  ( $i = 1, \dots, N$ ) verify the linear system

$$\frac{1}{\alpha_e^{(i)}} \frac{p_e^{(i)}}{\varepsilon_0} - \sum_{j \neq i} C_{i,j} \frac{p_e^{(j)}}{\varepsilon_0} = E_{\text{inc}}^{(i)} \quad (i = 1, \dots, N), \quad (4)$$

where we set  $E_{\text{inc}}^{(i)} = E_{\text{inc}}(\mathbf{r}_i)$ . By solving the above system it is possible to calculate the induced dipole moments, and in this way characterize the scattering properties of the system. In fact, using Eq. (2) and the asymptotic behavior of the Hankel function for large  $r$ , it is clear that the total scattered field in the far zone is

$$E_s^{\text{tot}}(\mathbf{r}) = k_0^2 \sqrt{\frac{2}{\pi k_0 r}} e^{i(k_0 r - \pi/4)} \sum_j e^{-ik_0 \hat{\mathbf{r}} \cdot \mathbf{r}_j} \frac{p_e^{(j)}}{\epsilon_0} \approx k_0^2 \sqrt{\frac{2}{\pi k_0 r}} e^{i(k_0 r - \pi/4)} \frac{p_{e,\text{tot}}}{\epsilon_0}, \quad (5)$$

where  $\hat{\mathbf{r}} = \mathbf{r}/r$  is the direction of observation, and  $p_{e,\text{tot}} = \sum_j p_e^{(j)}$  is the total electric dipole moment of the system. The last identity in Eq. (5) is valid when all the particles are within a relatively short distance (as compared to the free-space wavelength) from the origin, as will be assumed in what follows. In these conditions, the radiation pattern associated with the scattered field may be assumed uniform and the higher-order multipoles produced by the arbitrary distribution of polarization currents may be neglected. Consequently the total scattering linewidth of the system for plane-wave incidence (analogous to the total scattering cross section for two-dimensional problems) is such that

$$\frac{p_{e,\text{tot}}}{\epsilon_0} = -E_0 \frac{2\alpha_{e,\text{obj}}^{-1}[1 + \cos(k_0 d)] + \alpha_{e,s}^{-1} - 2C_1 - C_2 + 2C_0[3 + \cos(k_0 d)]}{4C_0^2 + \alpha_{e,\text{obj}}^{-1}(2C_1 + C_2) - \alpha_{e,\text{obj}}^{-1}\alpha_{e,s}^{-1}}, \quad (7)$$

where  $C_0 = k_0^2(i/4)H_0^{(1)}(k_0 d)$ ,  $C_1 = k_0^2(i/4)H_0^{(1)}(k_0\sqrt{2}d)$ , and  $C_2 = k_0^2(i/4)H_0^{(1)}(k_0 2d)$ .

In order to make the system effectively “transparent” to the incoming wave, it is necessary that  $p_{e,\text{tot}} = 0$  [see Eq. (6)]. Thus, Eq. (7) suggests that the condition of total transparency may be achieved provided the electric polarizability of the satellites is chosen such that

$$\alpha_{e,s}^{-1} = -2\alpha_{e,\text{obj}}^{-1}[1 + \cos(k_0 d)] + 2C_1 + C_2 - 2C_0[3 + \cos(k_0 d)]. \quad (8)$$

Notice that the right-hand side of the above equation depends exclusively on the electric polarizability of the object, on the frequency of operation, and on the distance  $d$ . To have a better feeling of the physical meaning of the transparency condition, let us consider the particular case in which both the satellites and the object have circular cross sections. The electric polarizability (along the axis of symmetry) of a cylindrical dielectric object with circular cross section and relative permittivity  $\epsilon$  and radius  $R$  is (see, for example, Ref. 15)

$$\alpha_e^{-1} = -i \frac{k_0}{4} \frac{1}{\epsilon - 1} \left[ -k_m \frac{J_0(k_m R)}{J_1(k_m R)} H_1^{(1)}(k_0 R) + \epsilon k_0 H_0^{(1)}(k_0 R) \right], \quad (9)$$

where  $k_m = k_0 \sqrt{\epsilon}$  and  $J_n$  is the Bessel function of the first kind and order  $n$ . When the particles are very subwavelength and  $k_0 R \ll 1$  and  $k_m R \ll 1$ , it is possible to approximate the above expression by<sup>15</sup>

$$Q \sim |p_{e,\text{tot}}|^2. \quad (6)$$

This analytical theory is completely general and it could be applied to a generic system with an arbitrary geometry and arbitrary number of (dipole-type) particles as long as their spatial distribution is over an electrically small cross section. We will relax this assumption in Sec. III, where we apply a full-wave analysis. In what follows, we restrict our attention to the configuration depicted in Fig. 1 formed by an object surrounded by four symmetrically positioned identical satellites. The distance between the object and the satellites is  $d$ . The electric polarizability of the object is  $\alpha_{e,\text{obj}}$ , whereas the electric polarizability of the satellites is  $\alpha_{e,s}$ . Assuming that the incoming field is a plane wave propagating along the  $x$  direction,  $E_{\text{inc}} = E_0 e^{ik_0 x}$ , and taking into account all the symmetries of the system, it is straightforward to solve the  $5 \times 5$  linear system [Eq. (4)] in closed analytical form. Detailed calculations show that the total electric dipole moment of the system is given by

$$\alpha_e^{-1} = \frac{1}{(\epsilon - 1)\pi R^2} - \frac{i}{4} k_0^2 + \frac{k_0^2}{2\pi} \left[ \gamma + \ln\left(\frac{k_0 R}{2}\right) \right], \quad (10)$$

where  $\gamma$  is the Euler constant. Thus, in the static limit  $\alpha_e^{-1} \approx 1/[(\epsilon - 1)\pi R^2]$ . It is also simple to verify that in the static limit ( $\omega \rightarrow 0$ ) the interaction constants vanish:  $C_0 = C_1 = C_2 = 0$ . Hence, in these conditions transparency condition (8) reduces to

$$\frac{1}{(\epsilon_s - 1)\pi R_s^2} = -4 \frac{1}{(\epsilon_{\text{obj}} - 1)\pi R_{\text{obj}}^2} \quad (\text{static limit}), \quad (11)$$

where  $\epsilon_s$  ( $R_s$ ) and  $\epsilon_{\text{obj}}$  ( $R_{\text{obj}}$ ) are the permittivities (radii) of the satellites and object, respectively. Notice that Eq. (11) may also be rewritten as  $4(\epsilon_s - 1)\pi R_s^2 + (\epsilon_{\text{obj}} - 1)\pi R_{\text{obj}}^2 = 0$ , which has a very intuitive meaning: it establishes that the transparency condition is achieved when the (spatial) average electric susceptibility of all particles in the system vanishes. This result is consistent with the discussions in our earlier works,<sup>1,10</sup> where it was shown that the transparency phenomenon stems from the annihilation of the electric dipole moments induced in the system.

Nevertheless, it should be emphasized that Eq. (11) is only valid near the static limit, and even for relatively small scatterers the frequency corrections are not necessarily negligible. These corrections may be taken into account by solving (with respect to  $\epsilon_s$ ) the exact transparency condition [Eq. (8)] with the electric polarizability given by Eq. (9). One important point is that in general the required permittivity for the satellites may be complex, even if the permittivity of the object is purely real. This effect is a consequence of the finite

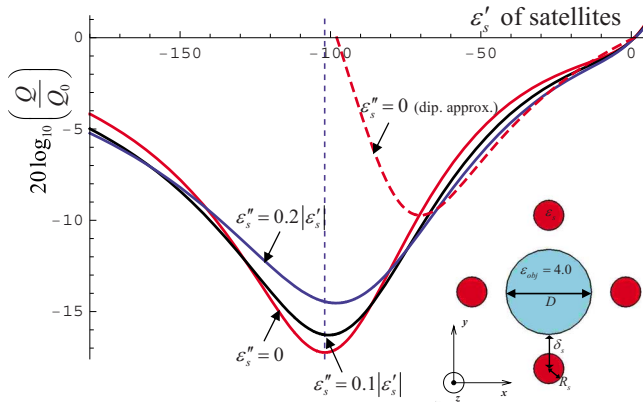


FIG. 3. (Color online) Total scattering linewidth  $Q$  for a 2D system formed by a circular object and four antiphase satellites (see the inset) as a function of the real part of the complex permittivity of the satellites,  $\epsilon_s = \epsilon'_s + i\epsilon''_s$ , and different values of the loss tangent.  $Q$  is normalized to the scattering linewidth of the object standing alone in free space,  $Q_0$ . The dashed vertical line represents the solution obtained using the GA. The dashed (red) line represents the result obtained using the dipole approximation in the lossless case.

electrical size of the particles and related field retardation [from Eq. (11), it is clear that in the static limit this situation cannot occur]. From the sign of the imaginary part in Eq. (10), it turns out that for relatively small configurations such as those considered here, some absorption loss in the satellites may yield further reduction in the scattering, and annihilate the total scattering from the system.

In order to validate the theory developed in this section, we have calculated the total scattering linewidth of a system formed by an object with permittivity  $\epsilon_{\text{obj}} = 4.0$  and diameter  $D = \lambda_0/6$  surrounded by four satellites ( $\lambda_0$  is the wavelength in free space at the operating frequency). The radius of the satellites is  $R_s = 0.05D$  and the distance between the center of the object and the center of the satellites is  $d = 0.6D$ . In Fig. 2 the total scattering linewidth is shown as a function of the real part  $\epsilon'_s$  of the complex permittivity of the satellites ( $\epsilon_s = \epsilon'_s + i\epsilon''_s$ ) and for different values of loss tangent. The solid lines were calculated using a dedicated (full-wave) method-of-moments (MoM) code, and fully take into account all the details of the structure and the effect of higher-order modes. The dashed lines were obtained by using the proposed analytical formalism [Eqs. (6) and (7)]. Notice that  $Q$  is normalized to the scattering linewidth  $Q_0$  of the object when the satellites are removed. It is seen that both sets of results concur well and predict that when the real part of the permittivity of the satellites is near  $\epsilon_s \sim -130$ , the scattering from the total system is drastically reduced. The small differences between the analytical and the numerical results (which are exacerbated by the logarithmic scale) are due to the effect of higher-order modes, which are neglected by the analytical model. It may be seen that the proposed cloaking mechanism is quite robust against the introduction of loss, and that the scattering strength of the combined object-satellites system remains much less than that characteristic of the isolated object, even when a significant amount of loss is added to the system. In this example, Eq. (8) predicts that the transparency condition is achieved with  $\epsilon_s = -120(1 - 0.03i)$ .

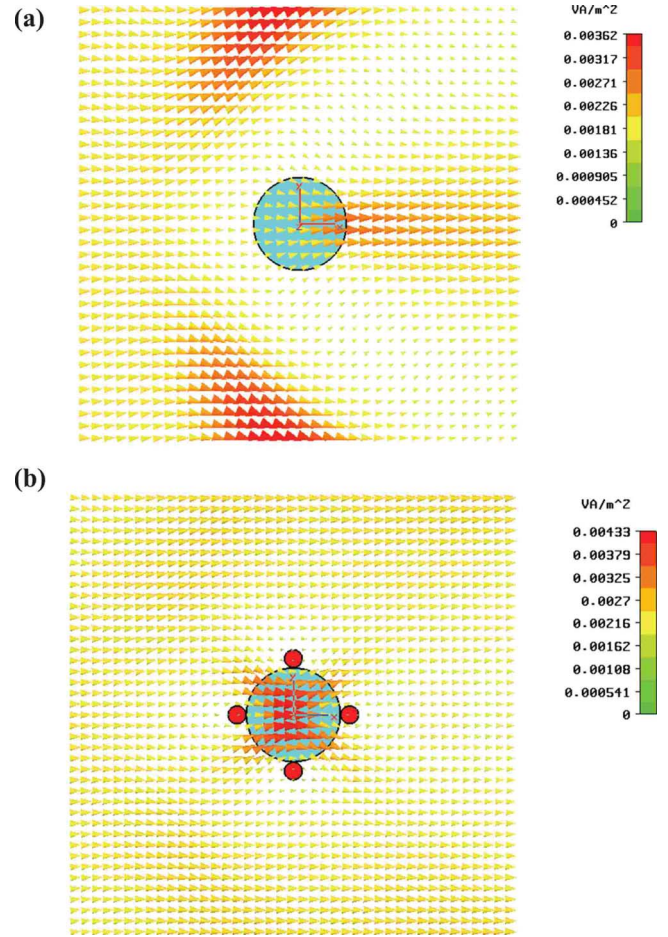


FIG. 4. (Color online) (a): Distribution of the real part of the Poynting vector when a cylindrical object standing alone in free space is illuminated by a plane wave. (b): Similar to (a) but the object is cloaked with four antiphase satellites, whose geometry and material parameters have been optimized using the GA.

Thus, the addition of a very small amount of loss to the system may improve the performance of the cloaking, effectively compensating for the dynamic coupling among the particles. This possibility will be demonstrated in Sec. III for a different, more general setup. It is interesting to note that the quasistatic transparency condition [Eq. (11)] predicts that the optimal permittivity of the satellites is  $\epsilon_s = -74$ , and thus obviously underestimates the value of the permittivity of the satellites. As discussed before, this happens because Eq. (11) is only valid very near the static limit, while in this example the diameter of the object,  $D = \lambda_0/6$ , and the corresponding field retardation are non-negligible.

The agreement between the analytical model and the full-wave simulations improves if the electrical size of the system is made smaller. On the other hand, when the size of either the satellites or the object becomes comparable to the free-space wavelength, the analytical model becomes significantly less accurate and one has to resort to full-wave numerical methods in order to determine a suitable configuration that may enable reducing the specific scattering of a given object. In Sec. III, we explore these possibilities employing a genetic algorithm (GA).

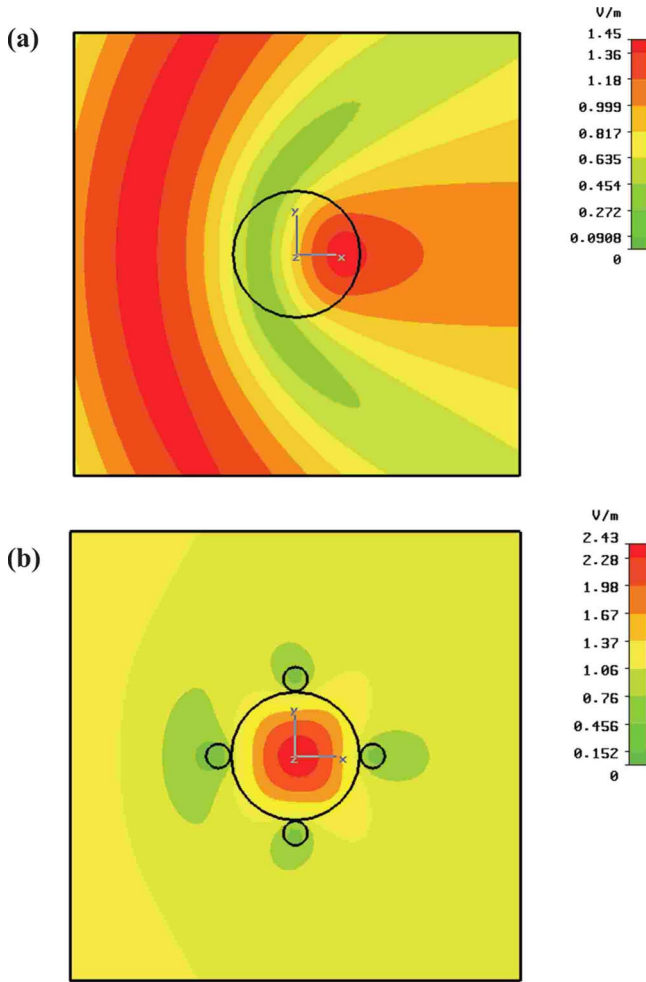


FIG. 5. (Color online) Distributions of the amplitude of the total electric field for the same scenario as in Fig. 4.

### III. OPTIMIZATION USING THE GENETIC ALGORITHM

Here we apply an optimization technique to calculate the relative position, size, and electromagnetic properties of the antiphase scatterers, in order to cause the invisibility of the overall system at the wavelength of interest. More specifically, for the configuration in Fig. 1, the objective is to calculate the permittivity  $\epsilon_s$ , the radius  $R_s$ , and the displacement  $\delta_s$ , which minimize the total scattering linewidth of the system. Unlike in Sec. II, the solution of the electromagnetic problem is full wave, and thus the method does not require anymore that the interaction between the different particles is limited to the dipole approximation. Moreover, a full-wave solution enables taking into account the contribution to the scattered field of all the multipoles, and thus the parameters of the antiphase satellites are tuned in order to minimize not only the scattering from the total electric dipole moment, but also the scattering from higher-order multipoles. In order to obtain a nearly isotropic response (independent of the direction of the incoming plane wave), we still suppose that the satellites are placed symmetrically around the object. For simplicity and without loss of generality, we will also assume that all the antiphase satellites are identical and have circular cross section, which is arguably the most interesting scenario from the point of view of a possible experimental demonstration of this phenomenon for geometries with high symmetry. The concepts proposed here may be easily generalized to the case in which the satellites are not identical, which may even provide further degrees of freedom for suppressing the possible residual scattering from the system, particularly in the cases for which the object to be cloaked is nonsymmetrical.

The GA is an adaptive search algorithm based on the evolutionary ideas of natural selection and biology.<sup>16</sup> Due to its versatility and generality, the GA is well suited to determine in an efficient manner the optimal solution of the problem

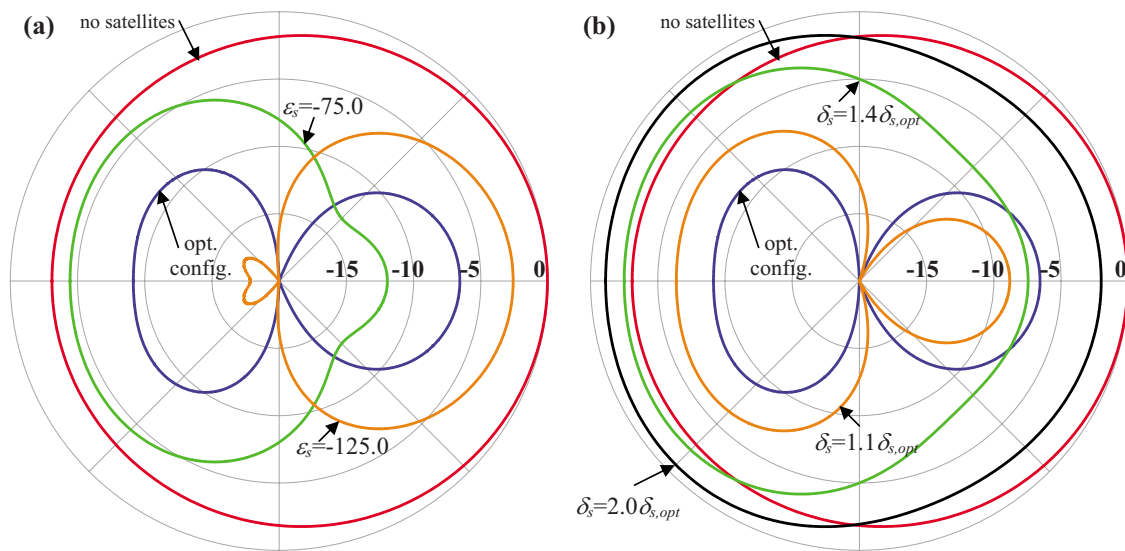


FIG. 6. (Color online) Radiation pattern in decibels (associated with scattered field) for different configurations of the considered system. The radiation patterns for the optimal configuration (blue line) and for an object isolated in free space (red line) are shown in both parts. (a): Radiation pattern for the case where the satellites are at the optimal distance from the object, but have nonoptimal dielectric constants  $\epsilon_s = -125.0$  and  $\epsilon_s = -75.0$ . (b): Radiation pattern for the case where the satellites have an optimal dielectric constant, but are located at distance  $\delta_s$  from the object different from the optimal distance  $\delta_{s,opt}$ .

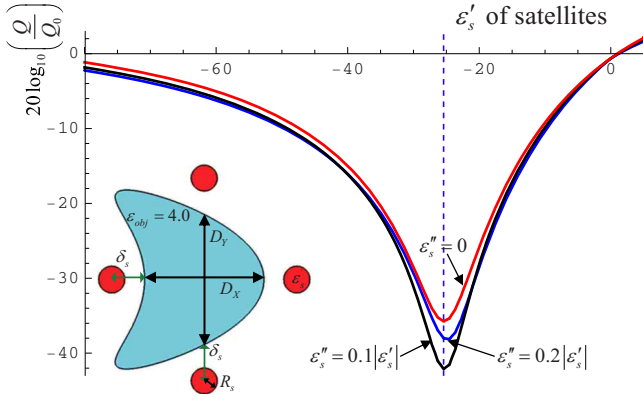


FIG. 7. (Color online) Total scattering linewidth  $Q$  for a 2D system formed by a kite-shaped object and four antiphase satellites (see the inset) as a function of the real part of the complex permittivity of the satellites,  $\epsilon_s = \epsilon'_s + i\epsilon''_s$ , and different values of the loss tangent.  $Q$  is normalized to the scattering linewidth of the object standing alone in free space,  $Q_0$ . The dashed vertical line represents the solution obtained using the GA.

under study. The GA approach is based on the evolution of an initial randomly generated population of candidate solutions (individuals) of the optimization problem. The variables to be optimized are coded into chromosomes which define the genetic code of each individual. A fitness function is used to sort the individuals in such a way that the best-ranking individuals are those that yield better solutions of the optimization problem. The initial population undergoes a selection process that mimics natural selection, ensuring the reproductive success of the most fit individuals (crossover) and possibly allowing for a low rate of mutations of the genetic code. In each generation, the worst-ranking part of population is replaced with offspring. The process is repeated iteratively, so that after some generations the initial population has evolved toward better solutions of the problem.

We have applied the GA to find an adequate configuration for the antiscattering satellites that brings down the scattering linewidth of the overall system. To this end, the parameters  $\epsilon_s$ ,  $r_s$ , and  $\delta_s$  were coded into 32 bits and associated with a chromosome, where by definition  $r_s = R_s / \delta_s$  ( $0 < r_s < 1$ ). Each individual in the population corresponds to a very specific value of the parameters  $\epsilon_s$ ,  $R_s$ , and  $\delta_s$ . The optimal solution was searched in a space of elements such that  $-200 \leq \epsilon_s \leq 10$ ,  $0.1D \leq \delta_s \leq D$ , and  $0.05 < r_s < 0.95$ , where  $D$  is the diameter of the object to be cloaked. For simplicity, we assumed in the optimization that the satellites are lossless. The fitness function was chosen equal to  $1/Q$ , where  $Q$  is the total scattering linewidth of the system for plane-wave incidence.  $Q$  was computed numerically using a dedicated method-of-moments code. The initial population had 180 individuals and was generated randomly. The mutation percentage was set equal to 5%. Typically, convergence was reached (or at least no further improvements were observed) after 40–50 generations.

In the first example, it was assumed that the diameter of the object is  $D = 0.25\lambda_0$  and the permittivity of the object is  $\epsilon_{\text{obj}} = 4.0$  (Fig. 1). (It is worth noting that although the diameter of the object is a fraction of the wavelength, i.e.,  $D$

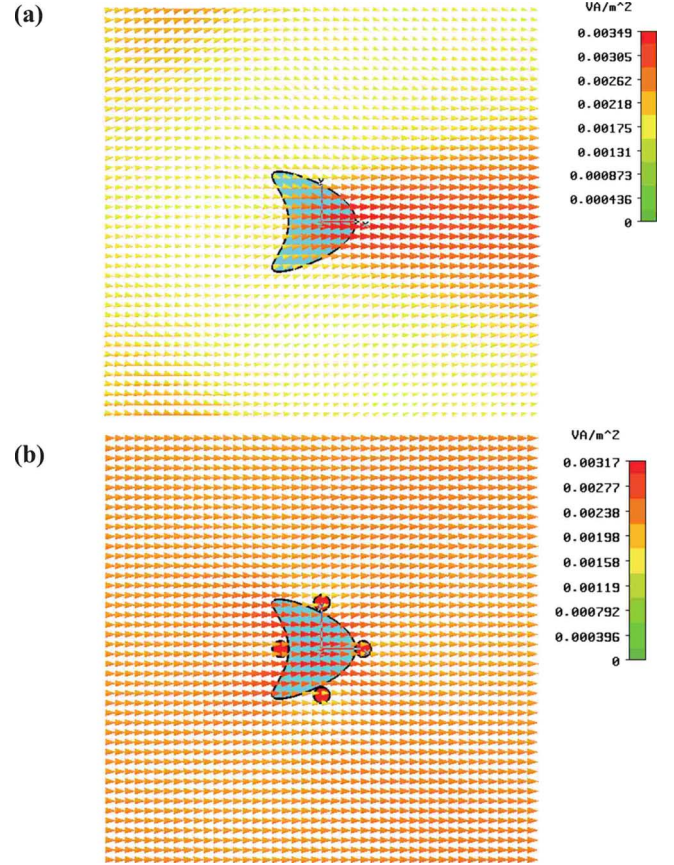


FIG. 8. (Color online) Similar to Fig. 4 but for a kite-shaped object.

$= 0.25\lambda_0$ , the dielectric object can still scatter significantly due to its size being near a resonance since the diameter is about half of the wavelength in the dielectric. Therefore, designing a cloak to drastically reduce this scattering would be useful for several applications). The GA yielded the following optimized parameters for the satellites:  $\epsilon_{s,\text{opt}} = -102$ ,  $\delta_{s,\text{opt}} = 0.10D$ , and  $R_{s,\text{opt}} = 0.094D$ . It is interesting to note that  $\delta_{s,\text{opt}}$  is very close to the lower bound of the considered interval of admissible solutions for  $\delta_s$ , whereas  $R_{s,\text{opt}}$  is very close to the upper bound of the interval of admissible solutions for  $R_s$ . A similar trend was observed in all the examples that we studied. It implies that the most advantageous configuration for the antiphase satellites is the one in which they are clustered very near to the object. The physical justification for this property stems from the fact that the optimal configuration for the antiphase satellites is such that the overall system remains as compact as possible. This ensures that the physical size of the overall system is kept comparable to that of the original object, and in particular minimizes the contribution of spurious higher-order multipolar components to the scattered field.

To give an idea of the variation in the scattering linewidth with the permittivity of the satellites (and also indirectly to study the bandwidth of the cloaking phenomenon), in Fig. 3 we plot  $Q$  normalized to the scattering linewidth  $Q_0$  of the object when the satellites are removed, as a function of  $\epsilon'_s$ , for different values of the loss tangent. It is seen that consis-

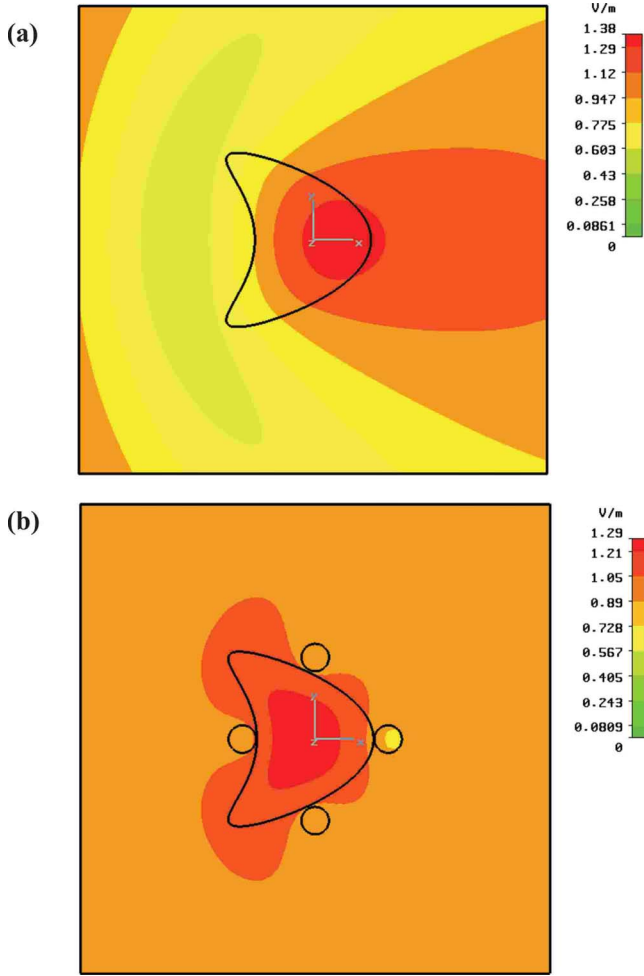


FIG. 9. (Color online) Similar to Fig. 5 but for a kite-shaped object.

tent with the solution of the GA, the scattering linewidth has a significant and broad dip at  $\epsilon_{s,\text{opt}} = -102$ . This demonstrates that the antiphase satellites effectively cloak the object, making it nearly invisible to an external observer. The broadness of the dip in the scattering linewidth confirms the nonresonant nature of this cloaking mechanism, consistent with the findings in Ref. 12. In accordance with the results in Sec. II, it is seen that the cloaking effect has a good tolerance to the effect of absorption loss. We have also plotted in Fig. 3 (dashed line) the response yielded by the analytical model derived in Sec. II [Eqs. (6) and (7)]. It is clear that the results predicted by the analytical model are too coarse and fail to describe accurately the properties of the system. This happens because the electrical size of the considered object is fairly large ( $D = 0.25\lambda_0 = 0.5\lambda_d$ , where  $\lambda_d$  is the wavelength in the dielectric).

To further validate the GA results, we have used CST MICROWAVE STUDIO™ (Ref. 17) to simulate the full-wave electromagnetic fields produced by plane-wave incidence at the frequency of operation. The distributions of the computed real part of the Poynting vector and the amplitude of the total electric field for an incident plane wave propagating along the  $x$  direction are presented in Figs. 4 and 5, respectively. Part (a) of the figures represents the case in which the object

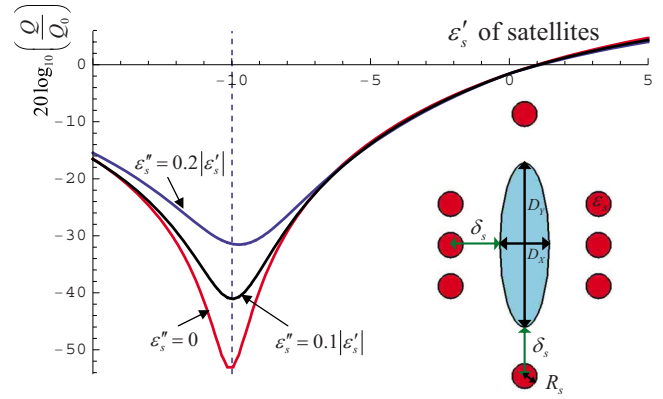


FIG. 10. (Color online) Total scattering linewidth  $Q$  for a 2D system formed by an elliptical object and eight antiphase satellites (see the inset) as a function of the real part of the complex permittivity of the satellites,  $\epsilon_s = \epsilon'_s + i\epsilon''_s$ , and different values of the loss tangent.  $Q$  is normalized to the scattering linewidth of the object standing alone in free space,  $Q_0$ . The dashed line vertical represents the solution obtained using the GA.

stands alone in free space, whereas (b) corresponds to the case of a cloak formed by antiphase satellites. The contrast between the two parts is striking: while in (a) the incoming wave is strongly scattered by the object, in (b) the electric field and the Poynting vector are nearly uniform away from the cloaking system, confirming that the antiphase satellites effectively cloak the object from the external field.

In Fig. 6 we depict the radiation pattern (associated with the scattered field) for different configurations of the considered system. In part (a), we study how the directivity and magnitude of the radiation pattern varies as the permittivity of the added satellites changes around the optimal value, assuming that the distance between the satellites and the object is the one obtained with the GA. As expected, the radiation pattern has typically a maximum along the  $x$  axis (the direction of the incoming wave). In part (b) we study the sensitivity of the radiation pattern when the distance  $\delta_s$  between the antiphase scatterers and the object is made different from the optimal value  $\delta_{s,\text{opt}}$ , keeping the dielectric constant of the satellites equal to the optimum value:  $\epsilon_s = \epsilon_{s,\text{opt}}$ . It is seen that the radiation pattern may vary significantly when  $\delta_s$  is changed, and that the scattering strength may increase very significantly when the satellites are displaced away from the object. This effect is caused by the increase in the overall physical size of the system, which enhances the effect of the higher-order multipoles and completely detunes the system.

In order to demonstrate the generality of the proposed cloaking mechanism and the fact that the described phenomenon is not specific for cylindrical objects with circular cross section, we have analyzed more complex geometries, such as the “kite”-shaped object depicted in Fig. 7. The permittivity of the object is the same as in the previous example, and the diameter of the object (along the  $y$  axis) is  $D_y = 0.14\lambda_0$ . Using the GA it was determined that the most advantageous parameters for the antiphase satellites are  $\epsilon_{s,\text{opt}} = -25.4$ ,  $\delta_{s,\text{opt}} = 0.12D_y$ , and  $R_{s,\text{opt}} = 0.11D_y$ . The plot of the scattering linewidth as a function of  $\epsilon'_s$  is shown in Fig. 7, for different

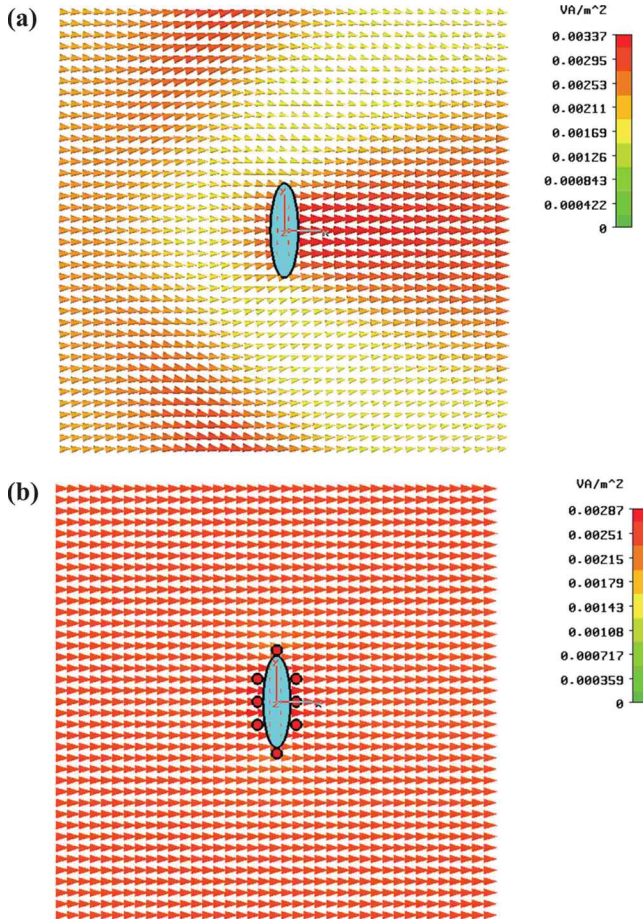


FIG. 11. (Color online) Similar to Fig. 4 but for an elliptical-shaped object.

values of the loss tangent. Quite interestingly, it is seen that in this example the effect of absorption loss in the satellites may help in reducing the scattering linewidth of the system. In fact, as discussed in Sec. II, in general the optimal value for the permittivity of the satellites is complex valued. We have verified numerically that at  $\epsilon'_s = -25.4$  the scattering linewidth decreases monotonically with increasing  $\epsilon''_s$  in the interval  $0 < \epsilon''_s < |\epsilon'_s|0.1$  (not shown here for brevity). The minimum  $Q$  is reached at  $\epsilon''_s = |\epsilon'_s|0.11$ . For  $\epsilon''_s > |\epsilon'_s|0.11$  the scattering linewidth increases monotonically with  $\epsilon''_s$  but remains smaller than the value of  $Q$  for  $\epsilon''_s = 0$  as long as  $0 < \epsilon''_s < |\epsilon'_s|0.23$ . Again, these results demonstrate the robustness of the proposed scattering-cancellation mechanism against the addition of loss, consistent with Ref. 12, which may, as demonstrated by this example, even further enhance the invisibility effect.

The representations of the real part of the Poynting vector and of the total electric field are shown in Figs. 8 and 9, respectively, for propagation along the  $x$  direction (lossless case). It is clear that despite the complexity of the considered object, the antiphase satellites can effectively annihilate the scattering from the object, making it transparent to the incoming field.

In a final example, we have considered a “needle-type” object with permittivity  $\epsilon_{\text{obj}} = 4.0$  and elliptical cross section, as illustrated in the inset of Fig. 10. The principal axes of the

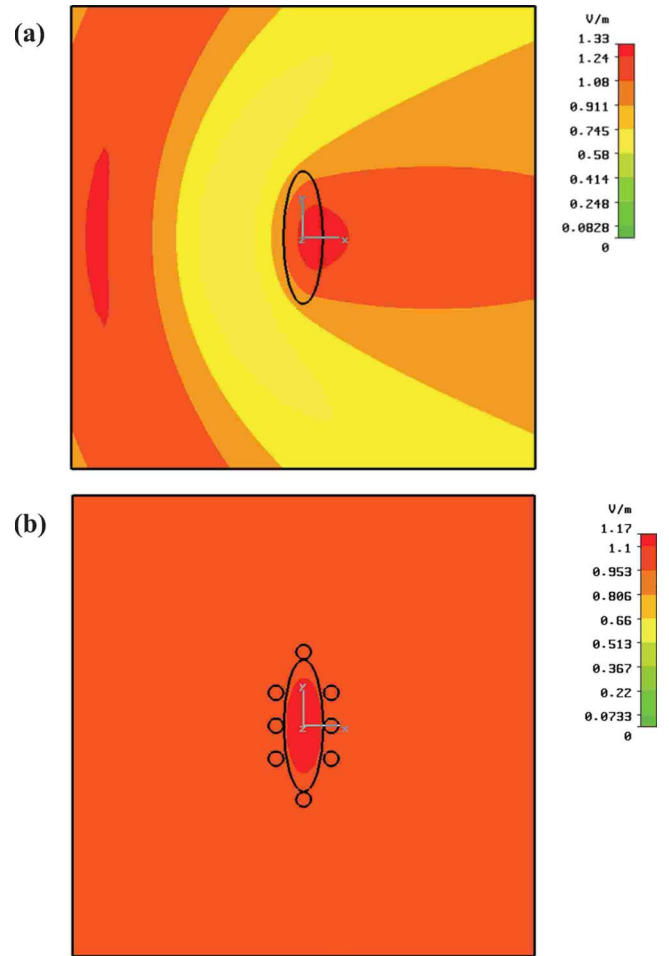


FIG. 12. (Color online) Similar to Fig. 5 but for an elliptical-shaped object.

ellipse are such that  $D_y = 0.25\lambda_0$  and  $D_x = 0.3D_y$ . The object is now surrounded by eight identical antiphase scatterers. The satellites are positioned at the points  $(\pm(D_x/2 + \delta_s), nD_y/4)$ ,  $n = -1, 0, 1$ , and  $(0, \pm(D_y/2 + \delta_s))$ , where the center of the coordinate system is coincident with the geometrical center of the object. Using the GA, it was found that a suitable set of parameters for the cloak is  $\epsilon_{s,\text{opt}} = -10.0$ ,  $\delta_{s,\text{opt}} = 0.060D_y$ , and  $R_{s,\text{opt}} = 0.055D_y$ . Not surprisingly, due to the increase in the number of satellites, the overall required negative permittivity for each satellite is lower in magnitude compared to the previous scenarios. The plot of the scattering linewidth as function of  $\epsilon'_s$  is depicted in Fig. 10, demonstrating a good tolerance to variations in the permittivity of the antiphase satellites around the optimal value and to the presence of material absorption. In Figs. 11 and 12 it is confirmed that the negative scattering provided by the satellites enables an overall reduction in the total scattering cross section of the system, and that the field distributions of the electric field and of the real part of the Poynting vector are nearly uniform, coincident with those of the incoming wave.

IV. CONCLUSIONS

In this work we have demonstrated that the cloaking mechanism presented in Ref. 1 may be generalized to the

case in which the cloak is formed by a set of suitable discrete scatterers (designated as satellites) surrounding the object. It has been verified that such conceptually simple and noninvasive cloaking solution may yield a dramatic drop in the scattering cross section for moderately sized objects and it has a good tolerance to the effect of loss. The relative position, size, and electromagnetic properties of the antiphase scatterers have been optimized using the GA. A larger number of antiphase scatterers may even provide more degrees of freedom for tailoring the way in which the cloaking phenomenon takes place for more complex-shaped objects. The large

number of degrees of freedom and the potentials of the GA technique may provide a viable way to cancel simultaneously multiple-scattering orders, creating an opportunity to extend this cloaking mechanism to electrically larger objects and collections of objects.

#### ACKNOWLEDGMENTS

M.G.S. was partially supported by “Fundação para a Ciência e Tecnologia” during his stay at University of Pennsylvania.

---

\*Author to whom correspondence should be addressed; engheta@ee.upenn.edu

<sup>1</sup>A. Alù and N. Engheta, Phys. Rev. E **72**, 016623 (2005).

<sup>2</sup>J. B. Pendry, D. Schurig, and D. R. Smith, Science **312**, 1780 (2006).

<sup>3</sup>D. Schurig, J. J. Mock, B. J. Justice, S. A. Cummer, J. B. Pendry, A. F. Starr, and D. R. Smith, Science **314**, 977 (2006).

<sup>4</sup>S. A. Cummer, B. I. Popa, D. Schurig, D. R. Smith, and J. Pendry, Phys. Rev. E **74**, 036621 (2006).

<sup>5</sup>W. Cai, U. K. Chettiar, A. V. Kildishev, and V. M. Shalaev, Nat. Photonics **1**, 224 (2007).

<sup>6</sup>U. Leonhardt, Science **312**, 1777 (2006).

<sup>7</sup>G. W. Milton and N. A. Nicorovici, Proc. R. Soc. London, Ser. A **462**, 3027 (2006).

<sup>8</sup>A. Alù and N. Engheta, J. Opt. A, Pure Appl. Opt. **10**, 093002 (2008).

<sup>9</sup>M. G. Silveirinha and N. Engheta, Phys. Rev. Lett. **97**, 157403 (2006).

<sup>10</sup>M. G. Silveirinha, A. Alù, and N. Engheta, Phys. Rev. E **75**, 036603 (2007).

<sup>11</sup>M. G. Silveirinha, A. Alù, and N. Engheta, Phys. Rev. B **78**, 075107 (2008).

<sup>12</sup>A. Alù and N. Engheta, Opt. Express **15**, 3318 (2007).

<sup>13</sup>A. Alù and N. Engheta, Opt. Express **15**, 7578 (2007).

<sup>14</sup>A. Alù and N. Engheta, Phys. Rev. Lett. **100**, 113901 (2008).

<sup>15</sup>M. G. Silveirinha, Phys. Rev. E **73**, 046612 (2006).

<sup>16</sup>Y. R. Sammi and E. Michielssen, *Electromagnetic Optimization by Genetic Algorithms*, Wiley Series in Microwave and Optical Engineering (Wiley, New York, 1999).

<sup>17</sup>CST MICROWAVE STUDIO™ 5.0, CST of America, Inc., www.cst.com